Detection of Moving Targets in the Visual Pathways of Turtles Using Computational Models

Neshadha Perera
Ronald C. Anderson
Department of Electrical and
Computer Engineering
Texas Tech University
Lubbock, Texas 79409–3102
Email: neshadha.perera@ttu.edu

Bijoy K. Ghosh
Department of Mathematics and Statistics
Texas Tech University
Lubbock, Texas 79409–1042
Email: bijoy.ghosh@ttu.edu

Abstract—**Microcircuits in the visual cortex of freshwater turtles have been revisited. These consist of a model of the retina, the lateral geniculate nucleus (LGN) and the visual cortex. In this paper, we present, via simulation how visual input on the retina is subsequently processed by the LGN leading up to an input to the cortex that generates a wave of activity. To gain access to the information content of the cortical wave, we analyze the extent to which these waves are able to discriminate the motion direction of the targets. The results are displayed in terms of root mean square error. We also show, via simulation, the role of the geniculate nucleus in terms of noise suppression. In particular, we show that, without the geniculate complex, retinal noise is strong enough to produce cortical activities without any form of target inputs. For realistic motion discrimination, it is imperative that noise in the geniculate is suppressed.**

Keywords—*Computational Neuroscience, Retina, Turtle, Visual Cortex, LGN, Motion, Target*

I. INTRODUCTION

This paper discuss the ongoing research work on neural models of the visual system of the freshwater turtles. The freshwater turtle visual system is similar to that of most vertebrates. In fact, all vertebrate retina share a similar structure (See [1] and [2]). Therefore, a turtle being a vertebrate can be used to study the vertebrate visual system. Furthermore, the structure of the turtle visual system has been extensively studied and detailed models were developed and successfully tested earlier.

A detailed model of the turtle's retina and a retinal patch is constructed [3] and a computational model for the lateral geniculate nuclei (LGN) was developed (See [4]).

A general discussion of the cerebral cortex of reptiles, including turtles is provided in [5], and a detailed discussion of the visual pathways in turtles is provided in [6]. Nenadic *et al.* in [7] provides a large scale model of the visual cortex.

A. Retina-Visual Cortex Model

The model of the Retina-Visual Cortex complex was developed initially without a complete model of the Lateral Geniculate Nuclei in between [8] in order to compare the
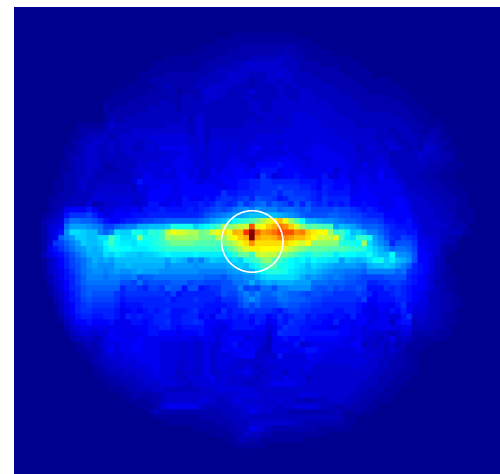
Fig. 1: Cell distribution of the turtle's retina. The white circle in the center of the retina represents the retinal patch used in this paper.

results of a model with LGN and study the effect of the LGN in the Turtle's visual cognition system.

The retina of the turtle's visual system consists of over 360,000 ganglion cells. However, the retinal model used in this paper consist of 520 ganglion neurons from a central patch in the visual streak of the turtle's retina [3]. The reduction of model into 520 cells was necessary in order to work with available computational resources. Figure 1 shows the location of the patch in the turtle's visual streak and the retina.

The retinal model consists of two types of ganglion cells which are intensity sensitive A-Cells and direction sensitive B-cells (See [3] , [9] and [10] for more details on the retina model) modeled using Hodgkin-Huxley equations (See [11]).

The visual cortex model was constructed with 744 neurons from a turtle visual cortex and a linear array of 201 LGN neurons is used to feed the synaptic currents to the visual cortex model. In this simulation study, a model in which the retinal cells connected to the visual cortex through the linear LGN cells in a linear fashion (See figure 2) was used.

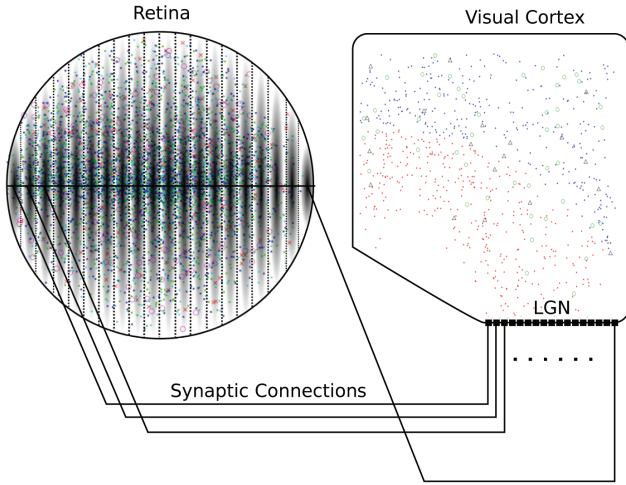Retinal cells were connected to the linear LGN cells of the

Fig. 2: Linear connection model. Black dots in the bottom of the visual cortex represents the cells in the linear LGN used to connect the two models. Only 17 out of 201 cells were shown in order to preserve the clarity of the figure.
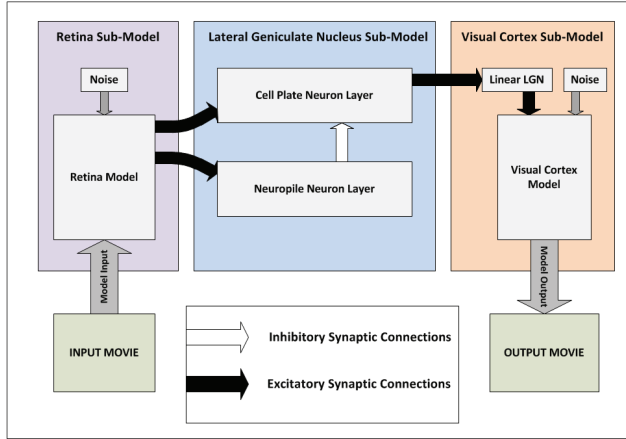

Fig. 3: The fused visual system model

Fig. 4: Mapping between LGC and visual cortex sub models

TABLE I: Synaptic connection strengths in retina-LGN-cortex model
(Key: $\multimap \bigcirc$: Excitatory connection, $\dashv \bigcirc$: Inhibitory Connection)

Retina $\multimap \bigcirc$ Cell Plates	9.0
Retina $\multimap \bigcirc$ Neuropiles	0.6
Neuropiles $\dashv \bigcirc$ Cell Plates	0.7
LGN $\multimap \bigcirc$ Visual Cortex	1.0

visual cortex model based on their x-coordinates. Cells in the left most vertical stripe of the retinal patch are connected to the first LGN cell in the linear array through synaptic connections. Cells in the next vertical stripe was connected to the second LGN cell in the linear array and this pattern continued until all the cells in the retinal patch was connected to the last LGN cell in the visual cortex model.

B. Retina-LGN-Visual Cortex Model

A model of the LGN was constructed and described in [4]. Comprising this LGN are 1166 Cell Plate and 112 Neuropile neurons, all modeled using Hodgkin- Huxley governed compartments and simulated using the GEneral NEural SImulation System. Inhibitory synaptic connections are formed from Neuropile cells to nearby Cell Plate neurons based on a 140-micron radius of influence.

Figure 3 shows the block diagram structure of the Retina-LGN-Visual Cortex Model. The LGN model is integrated with the same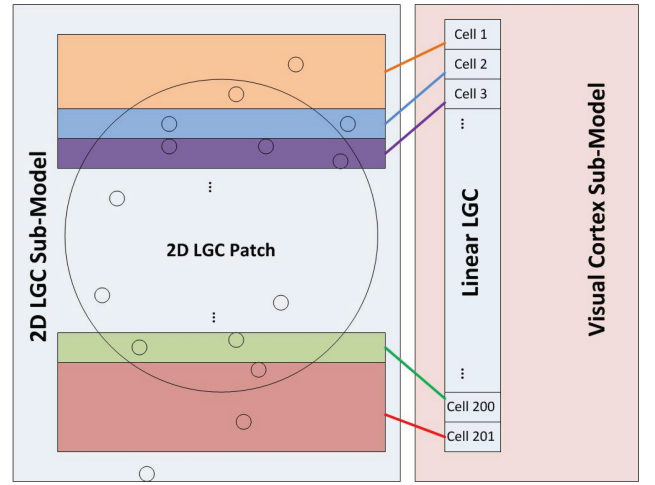 retina and visual cortex models as described in the previous section. General information flow is from the retina model through the LGN to the visual cortex model.

To connect the retina and LGN models, the retina patch is mapped to a 400-micron circular patch in the LGN model. This patch encompasses 501 Cell Plates and 36 Neuropile cells. Each Cell Plate neuron in the patch receives excitatory synaptic connections from all retinal ganglion cells within a 15-micron radius. All Neuropile neurons receive excitatory synaptic connections from ganglion cells within a 130- micron radius.

Connection of the LGN to the visual cortex model is achieved by dividing the LGN patch along the rostral-caudal axis into 201 strips. LGN Cell Plates residing in strip i form excitatory synaptic connections to member i of the 201 cell Linear LGN which serves as a front-end to the visual cortex model, as illustrated in the previous section. Figure 4 shows this connection procedure. It is important to note that the Neuropile cells do not exhibit synaptic connections into the visual cortex model.

Synaptic connection strengths from the retina model to the LGN were determined by progressive adjustment based on model response to Gaussian noise generated by the retina ganglion cells. Successful connection strengths were defined by LGN suppression of Gaussian noise signals from the retina, thereby preventing visual cortex response to noise in the retina model. For Gaussian retina noise of mean 0 and variance 3.0×10^{-11}, synaptic connection strengths given in table I were found to be effective.
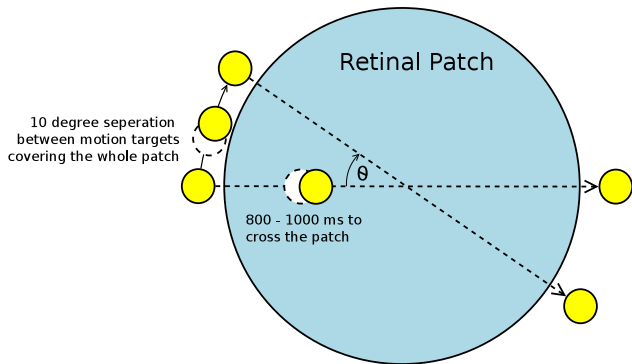
Fig. 5: Motion paths on retinal patch

II. SIMULATION SETUP & PARAMETERS

The simulation study comprised of simulating the two models individually for 1.5 seconds using GENESIS neural simulator software for a simulated light beam crossing the retinal patch at a constant speed. Retinal membrane potentials were recorded at each time step and later analyzed.

A zero mean and 3.0×10^{-10} variance Gaussian noise was introduced to the visual cortex of the retina-visual cortex model in order to perform the required statistical analysis. The retina however, did not had any noise level in this model.

It was observed that if any source of noise was injected into the retinal cells without the LGN being present, it causes the Visual Cortex wave being started without any input present in the retinal patch [8].

However, the model with LGN in the middle of the retinal-cortex connection is subjected to Gaussian noise at both retinal patch and the visual cortex. The retinal patch was injected with a zero mean and 3.0×10^{-11} variance Gaussian noise and the visual cortex was injected with zero mean and 9.0×10^{-10} variance Gaussian noise level.

Both models were simulated with a simulation step size of $5.0 \times 10^{-3}s$ using the GENESIS neural simulator for 30 iterations for each motion target. Motion path angle, which is denoted by θ was changed from $0°$ to $350°$ at $10°$ steps (See figure 5) making 36 different motion targets covering the entire retinal patch. Simulation was repeated 30 times for each motion path.

Figure 6 shows the ganglion cell membrane potential of the retinal patch as a movie for $0°$ motion path and the figure 7 shows the visual cortex cell membrane potential movie corresponds to the same $0°$ motion path.

III. PRINCIPAL COMPONENT ANALYSIS

Principal component analysis is primarily used to reduce the dimensionality of the data while retaining as much information as encoded in the original data set. This is done by transforming the observed data into a new set of uncorrelated variables [12]. Even though the original Karhunen-Loeve transformation is used for continuous variables [12], we will be using a discretized variant of the original Karhunen-Loeve transformation [13], [14].
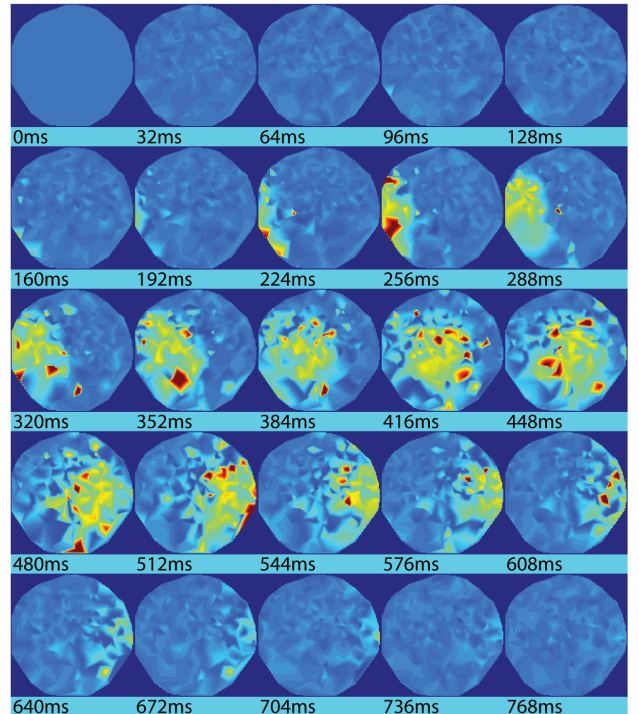

Fig. 6: Retinal activity movie for $0°$ motion path. The noise injected to the retinal model can be clearly seen as a light blue ripple in the movie frames. Areas with high cell membrane potential are represented in red color

The response waves in the visual cortex can be considered as a movie consisting a sequence of frames, each showing the visual cortex activity level in points in the visual cortex. The information encoded in these waves can be encoded by a two-step Karhunen-Loeve (KL) decomposition as described on Nenadic *et al.* [13] and Du *et al.* [14]

In this analysis, a two-step KL-decomposition was applied to the low pass filtered spike sequence with a *sliding encoding window*. As shown in figure 8, the time axis is covered by equal length, overlapping windows. The length of the sliding window remains constant $100ms$ while the starting and ending position of the window advances with time by steps of $10ms$. As shown in [14], each segment of the cortical response is mapped to a 6-dimensional principal component in the B-space which creates a sequence of points called a β strand when covered the whole simulation time.

Cortical responses from both retina-visual cortex model and retina-LGN-cortex model were used in PCA calculations and PCA points of the retinal responses from the latter model was also calculated for the sake of having a qualitative comparison.

IV. RMS DETECTION ERROR

We model the β coordinates as a realization of a Gaussian process, conditioned on the motion path angle and detect the target motion direction using the maximum likelihood estimator method [15].
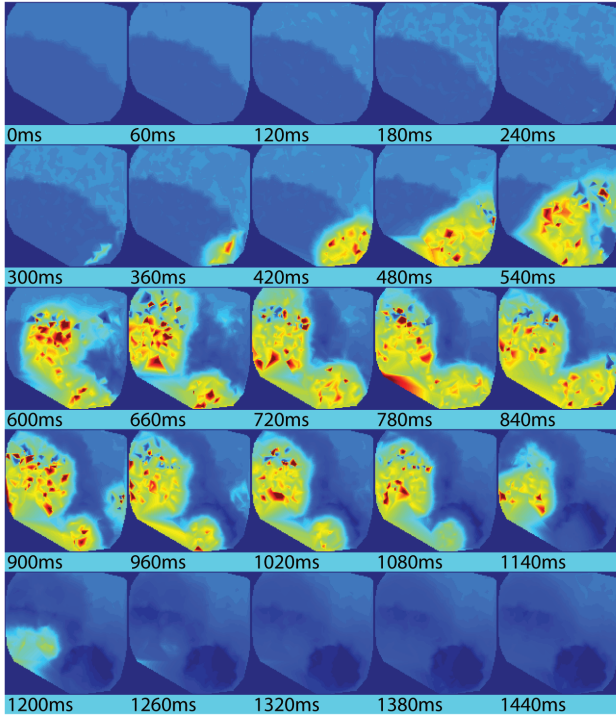
Fig. 7: Visual cortex activity movie for $0°$ motion path. The noise injected to the retinal model can be clearly seen as a light blue ripple in the movie frames. Areas with high cell membrane potential are represented in red color
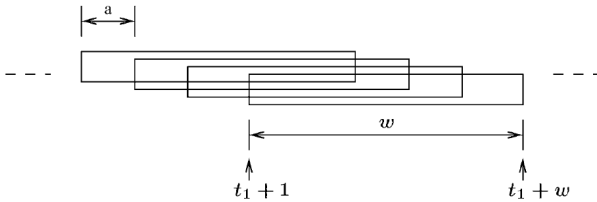

Fig. 8: Sliding encoding window technique

We formulate the null hypothesis H_0 as the sample of each dimension of β coordinates comes from a normal distribution vs. alternative hypothesis H_1 that it does not come from a normal distribution and use a 5% significance level for rejecting the null hypothesis [9] , [10]. This test is an adaptation of the Kolmogorow-Smirnov test [16] and do not require specifying the parameters of the target normal distribution. Failing to reject the null hypothesis imply that the samples come from a normal distribution.

The root mean square detection error is calculated using a repeated random sub-sampling validation with 30 iterations of the hypothesis testing. β coordinates from 25 randomly selected simulation repetitions were used at each iteration to train the algorithm and the remaining 5 was used to test and calculate the detection error. This process is iterated 30 times and the mean square detection error was calculated over the detection errors of all 30 iterations. The RMS detection error was calculated for cortical PCA points of both models and the
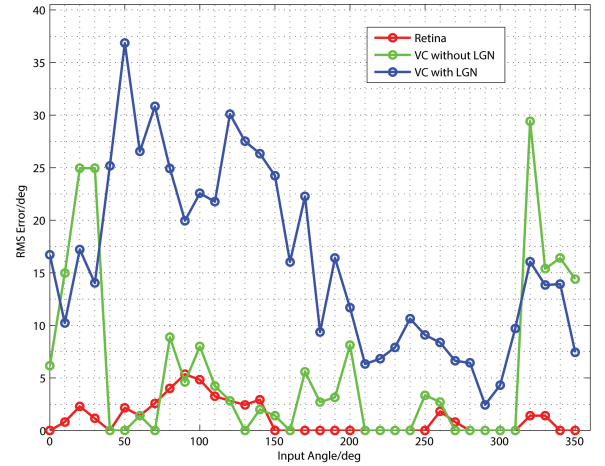

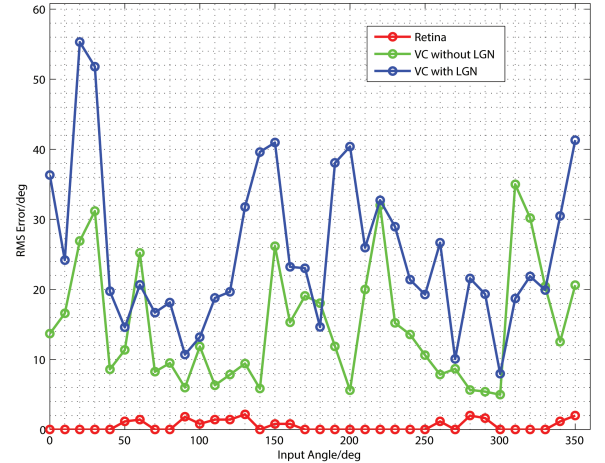Fig. 9: Mean square detection error at $t = 120ms$

Fig. 10: Mean square detection error at $t = 350ms$

retinal PCA points of the Retina-LGN-Cortex model.

V. RESULTS AND CONCLUSION

The mean square detection error of the two models along with the retinal patch is shown in figures 9, 10 and 11 for $t = 120ms$, $t = 350ms$ and $t = 500ms$ respectively. These three times are selected so that, it corresponds to the input is in the beginning, middle and at the end of the retinal patch. Here t is taken as the time after a wave started in a particular model. Since the wave starts at different simulation times in retina and cortex of each model, t is measured after synchronizing the wave starting times.

From figures 9, 10 and 11 the RMS detection error of the retina seems very low throughout the simulation. This result complies with the results given in [9] and [10] in a similar simulation setup. This means that the retina shows excellent motion path discrimination capability under noise. However, when the retina is connected to the visual cortex with or without LGN, and the cortical responses are used for the detection problem, it shows higher detection errors regardless of the model used.
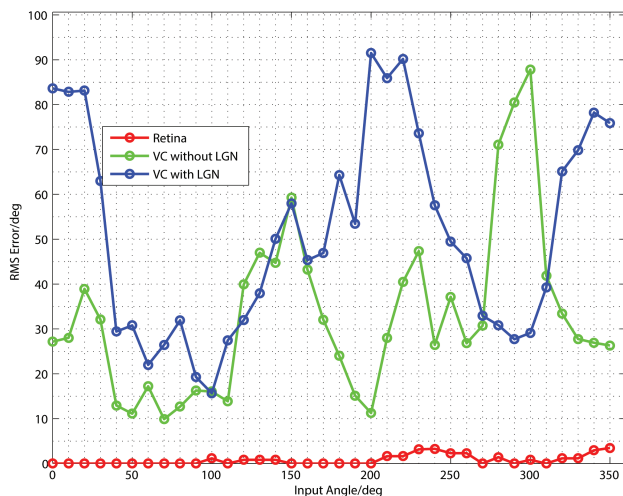
Fig. 11: Mean square detection error at $t = 500ms$

The RMS detection error plot at $120ms$ (Figure 9) does not show a stable error plot for the two visual cortex plots since the wave has just started in the visual cortex. This can be clearly seen from the visual cortex activity movie illustrated in figure 7 at the corresponding frame $360ms$. Similarly, at $500ms$ the cortical wave shows a bursting behavior over the entire visual cortex which seen in figure 7 at the corresponding frame $780ms$. The detection error tends to rise rapidly around this time.

The model without LGN shows a better detection accuracy over the model with LGN throughout the entire simulation time. However, there was no noise present in the retina in the model without LGN. Therefore the better accuracy does not necessarily imply that the model does a better job in discriminating motion targets under noise present in the retina. When there is noise present in the retina, the detection accuracy in the visual cortex is expected to be lower hence having high RMS errors. This can be observed from figures 9, 10 and 11.

On the other hand, the inhibitory nature of the Neuropile cells in LGN model is expected to reduce the effect of the retinal noise on the visual cortex. The noise present in the retina causes the visual cortex to produce waves even without any input [8] when connected directly without the LGN. Any motion target discrimination was not possible under that circumstance.

However, with LGN present in between Retina and the visual cortex, it was able to introduce noise in the retina and use the visual cortex for discriminating motion targets even with a higher RMS error. It is expected that the RMS detection error of the Retina-LGN-Cortex model could vary depending on the inhibition level used in the LGN.

A. Future Work

At this point, we are comparing the two models in order to investigate the function of the LGN in turtle's visual system. Therefore, this comparison study is expected to give only a qualitative comparison. Some of the model parameters including the connection strengths between retina, LGN and cortex sub models, noise levels in each sub model has to be fine tuned and the impact of each should be further studied in order to make a quantitative comparison.

REFERENCES

[1] J. E. Dowling, *The Retina: An Approachable Part of the Brain*. Cambridge, MA: Belknap Press of the Harvard University Press, 1987.

[2] R. D. Rodieck, *The First Steps in Seeing*. Sunderland, MA: Sinauer, 1998.

[3] M. P. B. Ekanayake, "Motion encoding and decoding in the turtle retina," Ph.D. dissertation, Department of Mathematics and Statistics, Texas Tech University, Lubbock, TX 79409, USA, July 2011.

[4] R. C. Anderson, "A model of the lateral geniculate complex of the turtle visual system: Noise suppression and target motion detection," Master's thesis, Department of Mathematics and Statistics, Texas Tech University, Lubbock, TX 79409, USA, December 2011.

[5] P. S. Ulinski, "The cerebral cortex in reptiles," in *Cerebral Cortex. Vol. 8A, Comparative Structure and Evolution of Cerebral Cortex, Part I*, E. G. Jones and A. Peters, Eds. New York, NY: Plenum Press, 1990, pp. 139–215.

[6] ——, "Neural mechanisms underlying the analysis of moving visual stimuli," in *Cerebral Cortex. Vol. 13. Models of Cortical Circuitry*, P. S. Ulinski, E. G. Jones, and A. Peters, Eds. New York, NY: Plenum Press, 1999, pp. 283–399.

[7] Z. Nenadic, B. K. Ghosh, and P. S. Ulinski, "Propagating waves in visual cortex: A large scale model of the visual cortex," *Journal of Computational Neuroscience*, vol. 14, pp. 161–184, 2003.

[8] M. A. P. N. Perera, "Target motion desctrimination with model retina and cortex," Master's thesis, Department of Mathematics and Statistics, Texas Tech University, Lubbock, TX 79409, USA, August 2011.

[9] B. K. G. Mervyn P. B. Ekanayake and P. Ulinski, "Decoding the speed and motion direction of moving targets using a turtle retinal patch model," *IEEE Transactions in Biomedical Engineering*, Unpublished.

[10] B. K. G. Mervyn P. B. Ekanayake, "Detection of motion direction of targets using a turtle retinal patch model," in *Mathematical System Theory - Festschrift in Honor of Uwe Helmke on the Occasion of his Sixtieth Birthday*, K. Huper and J. Trumpf, Eds. CreateSpace Publishers, 2013, pp. 115–125.

[11] A. L. Hodgkin and A. F. Huxley, "A quantitative description of membrane current and its application to conduction and excitation in nerve," *Journal of Physiology*, vol. 117, pp. 500–544, 1952.

[12] I. T. Jolliffe, *Principal Component Analysis*, 2nd ed., ser. Springer Series in Statistics. New York, NY: Springer, 2002.

[13] Z. Nenadic, B. K. Ghosh, and P. S. Ulinski, "Modeling and estimation problems in the turtle visual cortex," *IEEE Transactions in Biomedical Engineering*, vol. 49, no. 8, pp. 753–762, August 2002.

[14] X. Du, B. K. Ghosh, and P. S. Ulinski, "Encoding and decoding target locations with waves in the turtle visual cortex," *IEEE Transactions in Biomedical Engineering*, vol. 52, no. 4, pp. 566–577, April 2005.

[15] H. L. Van Trees, *Detection, Estimation and Modulation Theory, Part I*. New York, NY: John Wiley & Sons Inc., 1968.

[16] F. J. Massey, "The Kolmogorov-Smirnov test for goodness of fit," *Journal of the American Statistical Association*, vol. 46, no. 253, pp. 68–78, 1951.